

Response to Reviewers

Paper ID: JCOMP-D-22-00632

Authors: A. Panchal, S. H. Bryngelson, S. Menon

Title: A seven-equation diffused interface method for resolved multiphase flows

Date: October 19, 2023

Dear Prof. Adams,

We would like to submit a revised version of our manuscript entitled “A seven-equation diffused interface method for resolved multiphase flows”. We are thankful to you for guiding our manuscript through the review process, and to the reviewers for their comments, that has resulted in an improved paper content and for the readability of the manuscript. We have made every effort possible to address yours and the reviewers’ comments. We also worked on addressing your concern related to the novelty of this work (repeated below in *italics*).

All reviewers stress the issue of unclear novelty, in particular one reference is made to the earlier work of Tiwari. If the focus indeed is rather on a specific implementation, as rev. #1 and #2 indicate, it may be preferable to relay the submission to a more suitable journal. You may want to take particular care in addressing this issue should you decide to submit a revision.

The use of reduced approaches (e.g., five-equation model as in Tiwari et al. [1]) is well-established for modeling resolved multiphase entities (MPE) using diffused interface method (DIM). However, unlike the reduced models (e.g., [1]), the focus of this work is the seven-equation model that carries phase-independent pressures and velocities. The benefits of carrying phase-independent pressures are robust representation strong shocks and large density ratios, and the ability to use arbitrarily independent forms of the EOS for the phases, and carrying phase-independent velocities allows representation of both resolved and unresolved multiphase entities within the same modeling framework that would be beneficial for modeling dense-to-dilute multiphase flows. Below are the revised novel contributions of this work (re-emphasized in the paper):

- To demonstrate the unique potential of the more generalized seven-equation model, a new test (Section 4.4 in revised manuscript) is considered now. This contains unresolved particles in one part of the domain and the velocity non-equilibrium is required for accurate modeling of particle dispersion, whereas, a resolved multiphase interface is present in the other part of the domain that is modeled via DIM. This would not have been possible with the reduced five/six-equation models that enforce the velocity equilibrium analytically.
- To establish the use of the seven-equation model for modeling resolved MPEs, where the reduced models are already well-established, we show novel extensions to handle strong shocks and arbitrarily independent forms of EOS for the phases, viscous effects, surface tension, multiple species, and reactions within the same numerical framework. Here, the seven-equation model provides benefits over the five-equation model here by relieving the need to build a mixture EOS and due to the increased robustness.
- The seven-equation DIM may require additional algorithms for maintaining velocity and pressure equilibrium at the resolved interface, i.e., stiff relaxation (SR) solver, and interface compression techniques to limit the numerical diffusion of the interface. This aspect is also discussed.
- The limitations of the five/six-equation models and what the current 7-equation model provides are also discussed in this paper.

In addition to these, we have also worked on addressing the other concerns from the reviewers. Some key details are as below.

- We have addressed several concerns on validation of our results from reviewer-1 to the best of our ability. Additional simulations were conducted for the tests in Sections 4.1, 4.3, and 4.5 in the revised manuscript to address the reviewer's concerns. A comparison against past five-equation numerical results within the literature is added for the test in Section 4.8.
- A new test for the collapse of a spherical bubble (Section 4.6 in the revised manuscript) is considered as suggested by reviewer-1, and this provides further insights into the use of SR within the seven-equation framework.
- Several questions from reviewer-2 and reviewer-3 are addressed to justify our choice of methods, e.g., interface compression approach, HLLC Riemann solver, discrete equations method (DEM), etc.

In the following pages we provide detailed responses to each of the comments from the reviewers. The corresponding key text changes to the original manuscript are highlighted in red, blue, and magenta for the first, the second, and the third reviewer, respectively. The figures and the tables that are updated in the revised manuscript are highlighted by coloring their captions.

We hope this revision addresses all the reviewer comments and considered acceptable for publication in the Journal of Computational Physics.

Sincerely,
 Achyut Panchal
 Spencer H. Bryngelson
 Suresh Menon

Response to reviewer #1

The authors propose a numerical framework to solve compressible multi-phase flows using a 7-equation model with a DEM approach. This approach is rarely applied, however, it deserves attention due to its potential to generalize procedures for diffuse interface multi-phase flows. The authors provide numerical modeling for two dimensions and additional physical effects using well-established approaches in combination with the DEM model described by Abgrall and Saurel [2]. The verification of the proposed method is however limited in the manuscript (please see comments made below). The manuscript is well written. While the overall computational method is interesting, I do have a problem to fully appreciate the novelty of the procedure. Clearly, the combination of the presented methods is numerically challenging and deserves recognition. However, I fail to discern the appropriateness of this work for a general audience of JCP as no aspect of the numerics is new other than the combination of schemes. I understand that nobody has put together these different elements. The author indicate some additional application potentials of the described method. But what drawbacks from existing methods for the presented numerical examples in the manuscript are the authors trying to improve? There is no numerical analysis, and there is no direct comparison to state-of-the-art solvers demonstrating advantages of the proposed method. With this in mind I would suggest the authors consider a publication like Computer Physics Communications or similar. In summary, in the current form, I would not recommend accepting this manuscript, requiring a major revision. Please find below my additional comments.

We thank the reviewer for all the constructive comments, and the revisions, we believe have improved the readability and the technical content of the manuscript. All added clarifications to the points raised are indicated in red in the manuscript. Various concerns related to the validation of the proposed method are addressed individually below. Additional simulations are conducted for the tests in Sections 4.1, 4.3, and 4.5 in the revised manuscript for this. A comparison against past numerical results is added for the shock-droplet interaction test in Section 4.8. As suggested by this reviewer, an additional test, collapse of a spherical bubble, is considered to evaluate the effects of using the stiff relaxation solver within the seven-equation framework (Section 4.6 in the revised manuscript). The novelty statement of this work is revised in response to the comments, and a new test is considered in Section 4.4 of the revised manuscript to demonstrate the unique potential of the seven-equation model.

Updated novelty statement

Unlike the reduced models (e.g., [1]), the seven-equation model carries phase-independent pressures and velocities. Thus, both pressure and velocity non-equilibrium are allowed. For modeling resolved multiphase entities (MPE), compared to the well-established five-equation model, the benefits of carrying phase-independent pressures are the same as those of the six-equation model [3]. It can robustly represent strong shocks and large density ratios: $\rho^{(2)}/\rho^{(1)}, p^{(2)}/p^{(1)} \gg 1$. And furthermore, there is no need to formulate a mixture EOS, so one can use arbitrarily independent forms of EOS for the phases. The seven-equation model also retains phase-independent velocities, which is not expected provide a clear benefit for modeling resolved multiphase flows, where the velocity equilibrium is supposed to be maintained at the interface, but it will allow representation of dispersed unresolved MPEs, where the velocities relax towards each other in a finite time via specified drag laws (e.g., [4]). Such a capability can be of interest for dense-to-dilute multiphase modeling, e.g., liquid fuel injection [5], multiphase explosions [6], etc., where it is not computationally feasible to resolve all the small-sized MPEs (size \sim nm– μ m), but in other dense regions of the flow, certain multiphase features (size \sim mm–m) have to be resolved (e.g., for modeling primary breakup). Various algorithms that consider a rule-based transition between the vastly different resolved and dispersed phase approaches exist [7–9], however, unlike those, the seven-equation model will allow to handle both resolved and dispersed consistently within the same numerical framework with only minor changes related to the modeling of the relaxation terms.

After the initial development of the seven-equation model by Saurel and Abgrall [10], there have been relatively limited extensions and application use-cases [2, 11–14]. This appears to be due to the complexity of formulating an efficient numerical method and the lack of a clear establishment of the benefits of using a seven-equation model over the other well-established reduced approaches. This work is a step towards addressing these. To demonstrate the unique potential of using the seven-equation model over the reduced

models, a new test is considered. This contains unresolved particles in one part of the domain and the velocity non-equilibrium is required for accurate modeling of particle dispersion, whereas, a resolved multiphase interface is present in the other part of the domain that is modeled via DIM. Such modeling would not have been possible with the reduced five/six-equation models that enforce the velocity equilibrium analytically. To establish the use of the seven-equation model for modeling resolved MPEs, where the reduced models are already well-established, we start with the baseline DEM of Abgrall and Saurel [2] and show novel extensions to handle strong shocks and arbitrarily independent forms of EOS for the phases, viscous effects, surface tension, multiple species, and reactions within the same numerical framework. Here, the seven-equation model provides benefits over the five-equation model [15] by relieving the need to build a mixture EOS and due to the increased robustness. Finally, as noted earlier, the seven-equation DIM may require additional algorithms for maintaining velocity and pressure equilibrium at the resolved interface, i.e., stiff relaxation (SR) solver, and interface compression (IC) techniques may also be required to limit the numerical diffusion of the interface. Their need for the seven-equation model and for relatively complex configurations are not yet clear from the current literature, and it is evaluated in this work.

Corresponding changes are reflected in the revised manuscript on page-1 in the abstract, page-3 (line 72-86, 89-98, 99-109) in the introduction, and page 38 (line 926-930) in the conclusions.

Shock interaction with unresolved MPEs and a resolved interface (new test)

This test is considered to demonstrate the unique potential of the seven-equation model due to the velocity non-equilibrium that is allowed between the phases. As noted earlier, carrying phase-independent velocities can allow the same method to be used for modeling both resolved and unresolved multiphase flows. The configuration of this numerical test is created by combining the experimental setup of Rogue et al. [16], where a shock interacts with a bed of small-sized particles that cannot be resolved on the computational grid, with another setup considered earlier in Section 4.3 of this work, where a shock impacts on a resolved material interface. Dispersion of the unresolved particles has been modeled successfully in the past using dispersed phase approaches such as Eulerian-Eulerian (EE) or Eulerian-Lagrangian (EL) [4, 17], and the shock impact on a material interface also has been modeled using the reduced five/six-equation DIM [18], however, here, we model both with the same seven-equation model.

A shock tube of dimensions $6 \text{ m} \times 13 \text{ cm} \times 13 \text{ cm}$ is initialized with a Mach 1.3 shock at $x = 1 \text{ m}$, and a glass particle bed with particle radius $r_p = 750.0 \mu\text{m}$ and volume loading $\alpha^{(2)} = 0.65$ is placed at $x \in [2.00, 2.02] \text{ m}$. Initial pressure and temperature in the driven section ($x > 1 \text{ m}$) are 10^5 Pa and 298 K , respectively. Pressure in the driver section ($x < 1 \text{ m}$) is set corresponding to normal shock relations. Modifying the original experimental setup, a glass slab ($\alpha^{(2)} = 1 - \epsilon$) is placed from $x \in [4.00, 5.00] \text{ m}$, downstream of the unresolved particles. The computational domain is resolved with 3000 cells in 1D, resulting in a grid size of 2 mm. A symmetric boundary condition is used at $x = 0 \text{ m}$ and $x = 6 \text{ m}$ is set as a Neumann boundary condition. Both resolved and unresolved MPE are present in the same computational domain, and the same set of DIM Eq. 2.11 are solved everywhere. However, since the dispersed particles are not resolved on the computational grid, the velocity non-equilibrium between the phases in this region is modeled using a drag law. Correspondingly, in the region with dispersed particles, i.e., $x < 3 \text{ m}$, the velocity relaxation term in Eq. 2.12 is modeled as

$$\theta^u \Delta u_i = \frac{3\alpha^{(2)}}{8r_p} C_D \rho^{(1)} (u_i^{(2)} - u_i^{(1)}) |u_i^{(2)} - u_i^{(1)}|. \quad (0.1a)$$

Here, C_D is the particle drag coefficient that is computed as a correlation function of the particle Reynolds number Re_p following Crowe et al. [19]. For this test, the SR solver is not used in the rest of the domain, although it is possible to use it if needed in the regions away from the dispersed particles. This test is a first step towards demonstrating the potential of using the seven-equation model for both resolved and unresolved MPE, there are several improvements that will be needed in the future for its full applicability to problems of practical relevance.

- The dispersed particles and the resolved interface are well-separated for this test and they do not directly interact with each other. As a result, for the current demonstration, it is possible to use a drag law only for $x < 3$ m. For its use in real applications, a hybridization of θ^u may have to be considered so that it is dynamically determined based on the local conditions.
- As identified by Saurel et al. [17], the BN seven-equation model results in physically inaccurate wave-speeds for dispersed particles, and a corresponding hybridization of the volume-fraction evolution equation [17] may have to be considered for dense-to-dilute modeling.
- Some additional features that are included in this work, e.g., surface tension, interface compression, etc., may not be relevant in regions with unresolved droplets and they would have to be dynamically switched off in these regions with dispersed particles.

While acknowledging these limitations of the current demonstration, the simulation results are shown in Fig. 1. Stage-1 corresponds to $t = 2$ ms, when the initial shock (I) is yet to impact the dispersed particle curtain. Stage-2 corresponds to $t = 4$ ms, which is after initial shock (I) has impacted the dispersed particle curtain, and after the impact, a transmitted wave (T1) continues to propagate downstream (see Fig. 1(b)). A reflected wave (R1) is also generated and it propagates back upstream that is not shown here. Even though the SR for pressure is not used here, a pressure equilibrium between the phases is maintained at the particle curtain boundary as shown in Fig. 1(b) due to the DEM modeling of the non-conservative terms I^κ . A velocity non-equilibrium ($u^{(2)} - u^{(1)} \approx 50$ m/s) is observed in the dispersed particle region (see Fig. 1(e)), with the mixture velocity lying between the two phasic velocities. The specified drag law acts towards relaxing this difference in finite time. Capturing this velocity non-equilibrium and the corresponding particle dispersion would not have been possible with five/six-equation models that analytically enforce a velocity equilibrium.

To validate the interaction of (I) with the dispersed particle curtain, a comparison against experimental data is provided in Fig. 2. This includes pressure traces at three locations, 1 cm upstream of the initial particle slab-start location (point A), and 2 cm (point B) and 70 cm (point C) downstream of the slab-end location. Pressure values at points A and C are a result of shock reflection and transmission through the particle curtain. The pressure at point B, that is located immediately downstream of the initial particle bed, is strongly affected by the dispersion of the particles. The first jump in pressure at point A is due to incident shock, and the second jump is from reflection of this wave through the curtain. Pressure jump at point C at $t = 2$ ms is due to arrival of the transmitted wave through the curtain. The pressure transmission and reflection are predicted reasonably well using the seven-equation model. The particle curtain displacement is over-predicted, but this behavior is consistent with the results of Saurel et al. [17], where they show that these errors are due to physically inaccurate wave-speeds of the seven-equation model in the region with dispersed particles as previously noted.

The transmitted wave (T1) continues to propagate and hits the resolved material interface during stage-3 ($t = 6$ ms). This process is qualitatively similar to the shock impact discussed in the previous section, but the wave (T1) is significantly weak here due to its earlier interaction with the particle curtain. After the impact of (T1) with the resolved material interface, a transmitted wave (T2) propagates into the glass, and a reflected wave (R2) travels upstream back into the air (see Fig. 1(c)). Due to the high density (and therefore, high impedance) of the glass as compared to air, there is a negligible transmission of velocity into the glass (see Fig. 1(f)). Even though SR is not used here, the pressure and the velocity equilibrium are maintained at the interface due to the DEM modeling of I^κ .

These results are reported in the revised manuscript in Section 4.4, Figure 10, Figure 11. Related modifications are also included in the revised manuscript on page 14 (line 320), and Table 2 on page 18.

Some major comments:

- Introduction: An extended discussion on the benefits of the 7 equation model would be beneficial. Which applications do you have in mind where you assume velocity and pressure disequilibrium?

We thank the reviewer for this comment. This question is addressed in the updated novelty statement above. Corresponding changes are reflected in the revised manuscript on page-1 in the abstract, page-3 (line 72-86, 89-98, 99-109) in the introduction, and page 38 (line 926-930) in the conclusions.

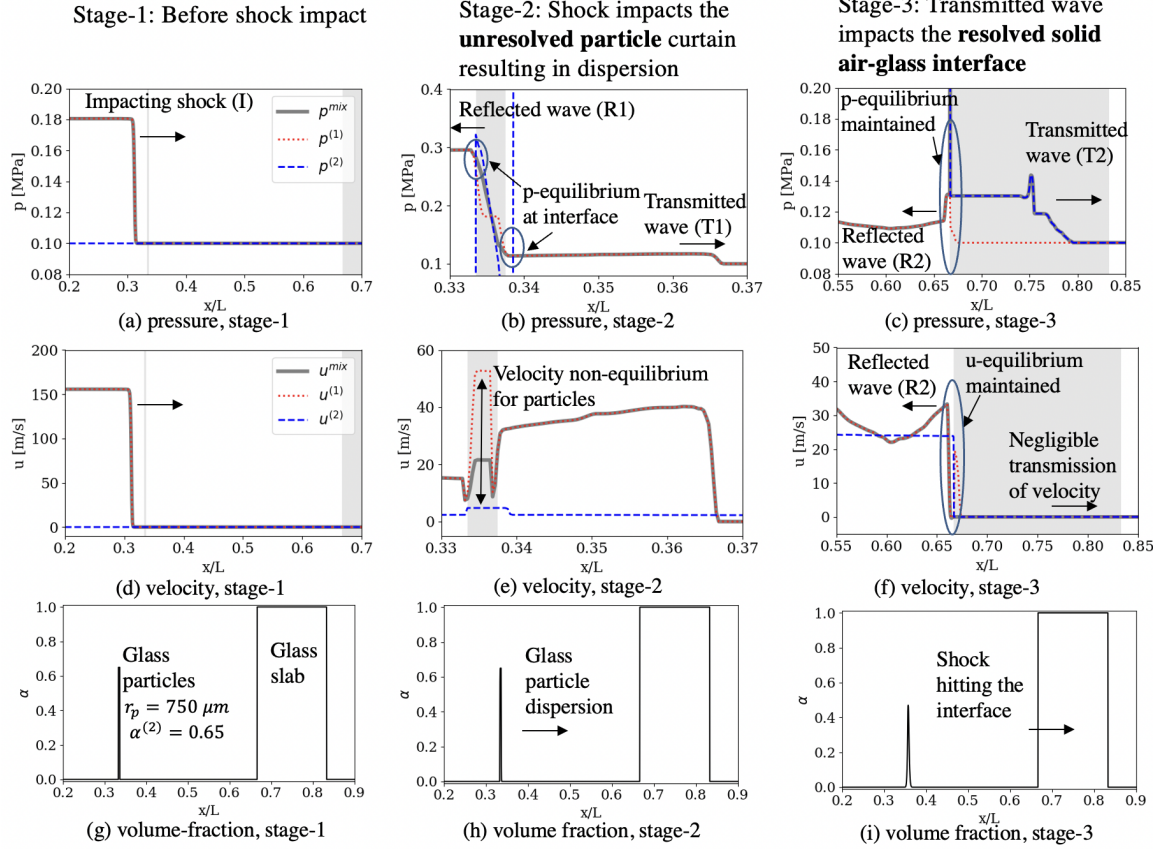


Figure 1: Results are shown for a shock interacting with dispersed and resolved multiphase entities within the same domain. The gray regions in subfigures (a-f) denote the presence of the particles or the glass slab.

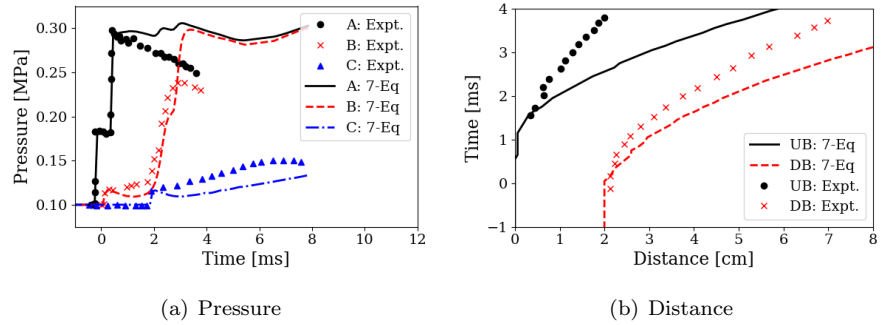


Figure 2: Simulation results for dispersed particle shock interaction with the seven-equation model are compared against experiments of Rogue et al. [16]. Subfigure (a) compares pressure traces at locations 1.89 m (A), 2.04 m (B) and 2.72 m (C), respectively. Subfigure (b) shows time evolution of upper and lower boundaries of the particle curtain.

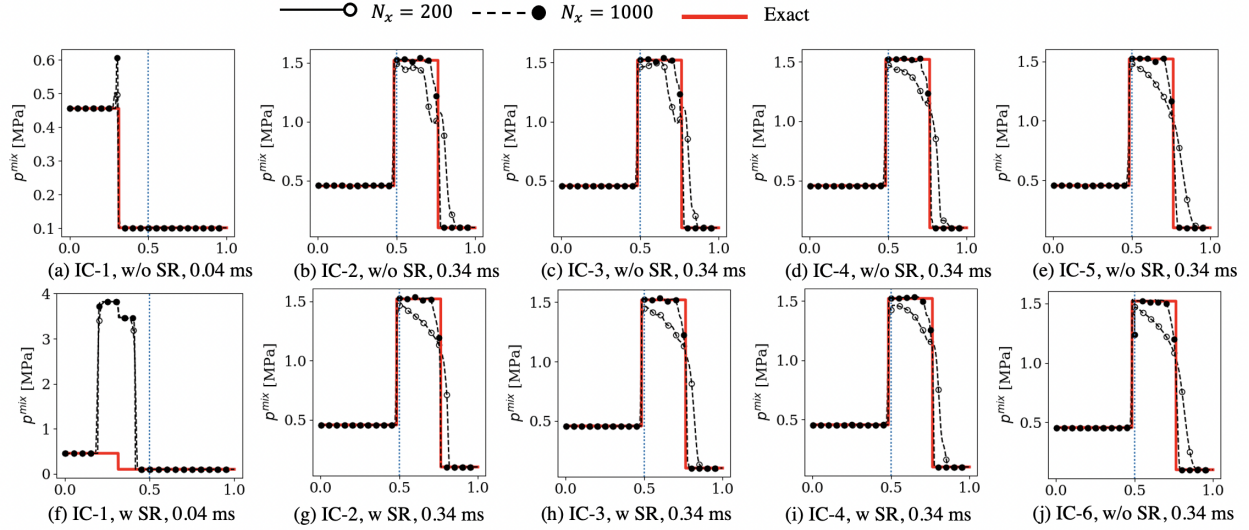


Figure 3: The p^{mix} is shown for the 1D shock interacting with Air/Al material interface. The vertical dashed line shows the location of the material interface. The results shown here are with the second-order scheme. The results for IC-1 are shown at an earlier time. Simulations with IC-5 and IC-6 with the SR were not possible and they are not shown.

- Why is 10^{-6} chosen for epsilon? Do lower values trigger numerical instabilities? You did not mention any problems with positivity in the manuscript. Did you experience any problems for more challenging cases?

Within the seven-equation framework, the evolution equations are solved for variables such as $\alpha^\kappa f^\kappa$. Here, f refers to phase-specific variables such as pressure p , velocity u_i , etc. Even small errors in $\alpha^{(\kappa)} f^{(\kappa)}$ (dependent on the numerical scheme) can amplify, as large errors in $f^{(\kappa)}$ with small $\alpha^{(1)}$, and it can lead to robustness problems when f^κ are used for equation of state, sound-speed computations, etc. Considering this, $\epsilon = 10^{-6}$ is retained here for most simulations in this work to be consistent with Abgrall and Saurel [2].

The effect of ϵ is evaluated further in Section 4.3 of the revised manuscript for the shock impacting a material interface. The following additional cases are considered

$$\text{IC-4 : } \epsilon = 10^{-12}, p^{(2)} = p^{(1)} \text{ and } u^{(2)} = u^{(1)} \text{ for } x/L < 0.3$$

$$\text{IC-5 : } \epsilon = 10^{-15}, p^{(2)} = p^{(1)} \text{ and } u^{(2)} = u^{(1)} \text{ for } x/L < 0.3$$

The simulation results are reported in Fig. 3. The predictions for $\epsilon = 10^{-6}, 10^{-9}, 10^{-12}$ (IC-2, IC-3, IC-4) are similar to each other both with and without a relaxation solver. At the lower limit of ϵ , the simulations with $\epsilon = 10^{-15}$ are able to predict the mixture quantities (p^{mix}, u^{mix}) without the relaxation solver, but the phase-specific pressure of the gas-phase, i.e., $p^{(1)}$, shows a spike (~ 0.2 MPa) in the liquid-phase region (not shown here) that can lead to a crash in the EOS solver for more complex problems. On the other hand, the simulation with $\epsilon = 10^{-15}$ with the SR fail at the first step due to the failure of the iterative solver. Considering this, the choice of $\epsilon = 10^{-6}$ is justified for the other cases, although the results show that using $\epsilon = 10^{-9}, 10^{-12}$ is also possible.

We did not encounter any problems with positivity of volume-fractions for any of the complex cases considered in this work.

The corresponding changes in the revised manuscript are reflected on page 17 (line 442-447), page 21 (line 509-510, 540-546), and Figure 7.

- Have you considered to limit each phase to the area of interest? For multiple phases it seems not practical to evaluate each phase in the whole domain.

We have not considered the possibility of limiting each phase to its area of interest in this work. Such a development may be of interest to reduce the computational cost of the seven-equation model. However, considering the numerical challenges that may arise to achieve this while still maintaining the mixture conservation and hyperbolicity property of the model, particularly when different variables are active on different sides of the diffused interface, this can be addressed in a future work.

No corresponding changes are made in the revised manuscript.

- Case 4.3.: Can you comment on the weak performance around the transmitted wave for moderate resolutions ($N=200$). This seems to be a crucial drawback for multi-dimensional simulations since you often cannot afford very high resolutions.

The coarse-grid prediction ($N_x = 200$) shows noticeable errors in the transmitted shock, but the results improve with grid refinement. This is a challenging test due to the high density ratio ($\rho^{(2)}/\rho^{(1)} = 2320$) at the material interface on which the shock is impacted. As per the authors' knowledge, other multiphase modeling predictions for this configuration are not available in the literature for a one-to-one comparison. However, such comparison is now included in the revised manuscript for a 2D shock-droplet interaction test. Either a higher-order extension of the discrete equations method (DEM), or an adaptive mesh refinement (AMR) can be considered in the future to improve the solution accuracy.

For the coarse grid ($N_x = 200$), with $\epsilon = 10^{-6}, 10^{-9}$ (IC-2, IC-3), without the SR, the predictions do show numerical oscillations in the transmitted shock, whereas, the lower ϵ values (IC-4, IC-5) and the simulations with the SR show primarily diffusive errors. The predictions improve for the fine grid. This can be attributed to errors in modeling the non-conservative interface terms I^κ , since in absence of the relaxation terms, they are entirely responsible for handling the interphase exchange and maintaining the pressure and the velocity equilibrium.

The corresponding changes are reflected in the revised manuscript on page 21 (line 524-529, 549-553).

- Case 4.4 2 does not seem to be very convincing, errors are raising with resolution and SR does not seem to work properly in combination with surface tension.

The DEM modifications in the surface tension are designed so that a pressure jump is handled across the (1)-(2) interface, whereas the (1)-(1) and the (2)-(2) interfaces should behave as before. As expected, the case with the SR maintains pressure equality away from the interface and enforces a pressure jump between $p^{(1)}$ and $p^{(2)}$ within the numerically diffused interface. However, because of this, pressure jumps are present even in the phasic fields $p^{(1)}$ and $p^{(2)}$ near the boundaries of the diffused interface. They result in pressure jumps at the (1)-(1) and the (2)-(2) interfaces within the DEM (in addition to the jump at (1)-(2) interface which is expected), possibly causing these larger errors. The results suggest not using the SR and using the interface compression as the optimal choice, while modeling surface tension effects within our seven-equation numerical framework.

Even for that, the errors in p^{err} and KE^{mix} do not necessarily reduce with the grid, and this has also been observed in a past work [13]. This could be due to contrasting effects; as we would compute the curvature more accurately for the finer grids, however, the coarser grids would help the parasitic currents to diffuse numerically. An updated error measure, L_2 norm of the mixture pressure p^{mix} is computed as

$$L_2 = \sqrt{\frac{1}{\sigma\beta} \int_{\Omega} (p^{mix} - p^{exact})^2}, \quad (0.2)$$

where p^{exact} is p_{atm} for $r \geq r_0$ and $p_{atm} + \sigma\beta$ for $r < r_0$. The errors in L_2 , that have been used in the past to show grid convergence [13], do consistently reduce with grid refinement for the simulations without the SR and with the interface compression, but not for the other options (see Table 1).

Corresponding changes are made in the revised manuscript on Page 26 (lines 655, 663, 669-672) and Table 3.

- Case 4.4 3: Fig. 12: There is a noticeable offset in oscillation frequency. Can you comment on reasons for this?

Table 1: Errors L_2 for the circular droplet surface tension test are shown for various grids and various simulation options. Simulation results without the stiff relaxation solver (SR) and with the interface compression (comp.) are highlighted as they show the lowest errors.

Case	200×200	400×400	800×800
L_2 [Pa]			
w/o SR, w/o comp.	6.57×10^1	8.87×10^1	7.22×10^1
w SR, w/o comp.	2.58×10^2	3.45×10^2	3.84×10^2
w/o SR, w comp.	6.61×10^1	4.83×10^1	4.41×10^1
w SR, w comp.	1.09×10^2	2.96×10^2	2.46×10^2

Table 2: Errors in predicted oscillation frequency (ω) for droplets with surface tension. Results are only reported here for the case without SR and with interface compression.

Case	Error in ω prediction
200×200	66.0%
400×400	34.0%
800×800	7.89%
1600×1600	5.89%
2400×2400	3.89%

The previous simulation results were gathered after every $0.2t_{osc}$. We redid these simulations with output files written every $0.02t_{osc}$ to obtain a better comparison against the exact oscillation frequency. The updated results are shown in Fig. 4. Since the pressure field is initialized uniformly, it takes approximately $0.05t_{osc}$ the pressure to develop within the domain and the oscillation sequence to set in. Accordingly, the simulation results are shifted on the time-axis such that the first crest in Fig. 4 matches with $0.5t_{osc}$ (first vertical line). Furthermore, the resulting errors in the computed oscillation frequency with respect to its exact value are reported in Table 2 for different grids. The errors are larger for the coarser grids, but reduces to $< 8\%$ for grids larger than 800×800 .

Corresponding changes are reflected in the revised manuscript on page 28 (lines 693-696, 701-703), Figure 15, page 39 (line 951) and Table 4.

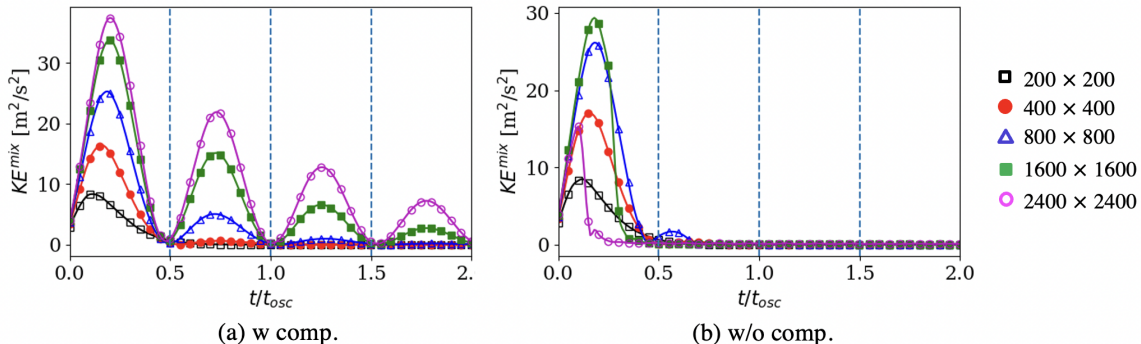


Figure 4: KE^{mix} [$\text{kg m}^2/\text{s}^2$] for an oscillating ellipsoidal droplet. The dashed vertical lines correspond to the exact oscillation period. The simulation results have been shifted by $0.05t_{osc}$ on the bottom axis to exclude initial transients.

- There are some disturbances visible behind the shock wave in Fig 16b. Do simulations w/o SR results trigger such disturbance even for simple shock wave propagation?

Disturbances are noticeable behind the propagating shock in the Numerical Schlieren ($|\partial\rho^{(1)}/\partial x_i|$), particularly without the SR at $\tau = 0.03$ (Fig. 20(b) in revised manuscript). However, the corresponding disturbances in terms of the primitive variables are very small, e.g., for $\rho^{(1)}$, they are $\sim 0.02\%$ without the SR and $\sim 0.09\%$ with the SR, and they can be considered errors related to the numerical scheme.

This is noted in the revised manuscript on page 33 (line 823-825).

- Case 4.6: Assumption of inflow condition influence should be verified by a simulation. Please provide references for the statement “Similar errors have been observed in earlier numerical studies”. I understand that quantitative validation of experimental measurements is a difficult task. However, it is hard to judge the quality of a proposed method if results differ to this extend.

Unfortunately, it was not possible to update the inflow conditions in our seven-equation approach and this can be considered in the future, however, to provide a comparison of our approach against the available numerical studies, we now compare our predictions against those of Chen [20] and Meng and Colonius [21]. These are shown in Fig. 5, Fig. 6, Fig. 7, and Fig. 8. There are certain differences in the simulation approach. Chen [20] used free-stream boundary conditions with $N_x = 48$, and Meng and Colonius [21] used characteristic-based non-reflective boundary conditions [22] and $N_x = 100$. Both these studies used the five-equation model. The current study uses the seven-equation model and simplified subsonic characteristic-based boundary conditions [23] that treat the liquid-phase quantities as passive scalars (see Section 3.7 in the revised manuscript). The grid resolution $N_x = 83$ from the current simulations is the closest to [21]. Below are some conclusions

- The droplet leading edge (x_L/d_0) evolution is shown in Fig. 5. Our results initially ($\tau < 0.7$) match with those of Meng and Colonius [21] and the experiments [24], but later on diverge away from it, while coming closer to those of Chen [20].
- Without the SR and without the interface compression, the predicted droplet width w matches well against the data (<5% error) for all grid resolutions. These results also comparable with Meng and Colonius [21].
- The droplet height d is grossly underpredicted at coarser resolutions, and a grid convergence is obtained only for $N_x \geq 255$. Still, the current results with $N_x = 83$, $\alpha_T^{(2)} = 0.9$ are closer to $N_x = 100$, $\alpha_T^{(2)} = 0.99$ of Meng and Colonius [21], whereas, the grid converged results for $N_x = 170, 255, 340$ lie between the two limits of $\alpha_T^{(2)} = 0.25 - 0.99$ in [21].
- The droplet area is expected to reduce with time for the experiments due to the stripping of small-sized droplets. A grid convergence is obtained for $N_x \geq 170$, and the finer grids’ results match the measurements [24] and the previous numerical results [21] with <5% error.

The corresponding changes are reflected in the revised manuscript on page 34 (lines 844-849, 854, 861, 865-867, 870), page 39 (line 954) in the text and Figures 21-24.

- An interesting additional case study should be considered concerning the prediction of the Rayleigh collapse. Schmidmayer et al. [25] recently started a discussion about the influence of relaxation on the collapse behavior. It would be interesting to evaluate the behavior of the proposed method, especially, in context with the discussed relieved need of SR.

This test-case is now included (Section 4.7 in the revised manuscript), and it does provide new insights into the usage of the stiff relaxation solver with the seven-equation model. We thank the reviewer for this suggestion. The obtained results are as below.

Computing collapse and rebound of a spherical bubble surrounded by a high-pressure liquid is a seemingly simple but challenging problem, where, instead of a wave impacting a multiphase interface, the waves are generated at the interface [25, 26]. Modeling the pressure (or mechanical) equilibrium is crucial for obtaining accurate predictions for this test. As a result, the five-equation model without the volume fraction source term [27] showed inaccurate results, and the augmented model of Kapila

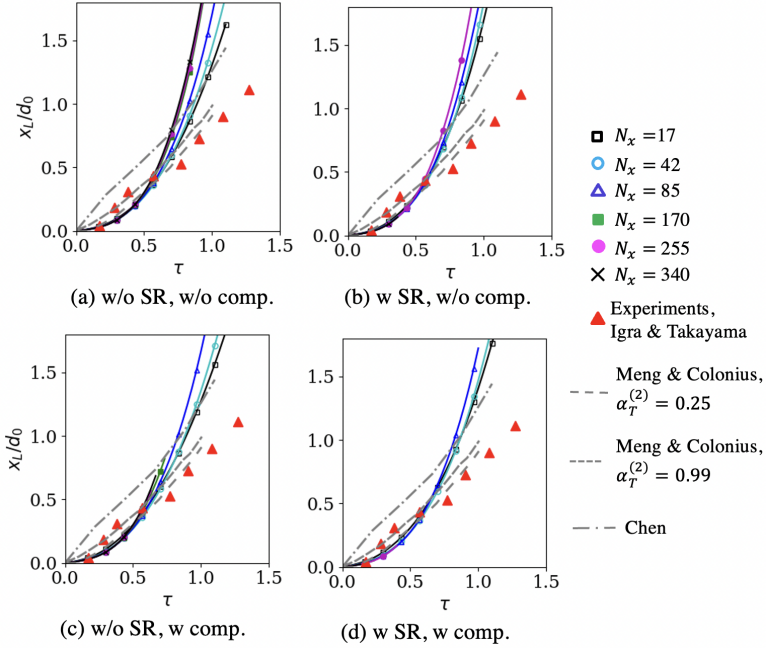


Figure 5: Time-evolution of the droplet leading edge (x_L) compared against the experimental measurements of Igra et al. [24] and numerical results of Meng and Colonius [21] and Chen [20].

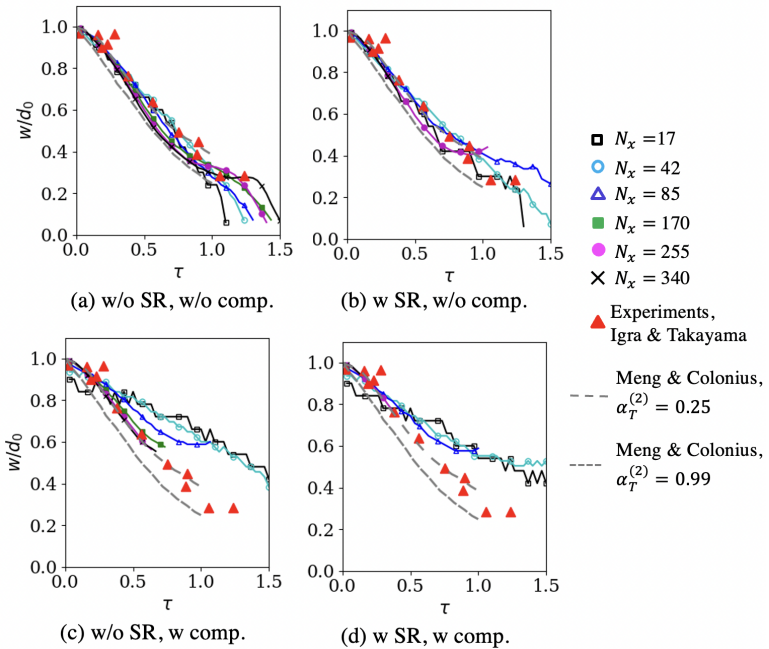


Figure 6: Time-evolution of the droplet width (w) compared against the experimental measurements [24] and a previous numerical study [21].

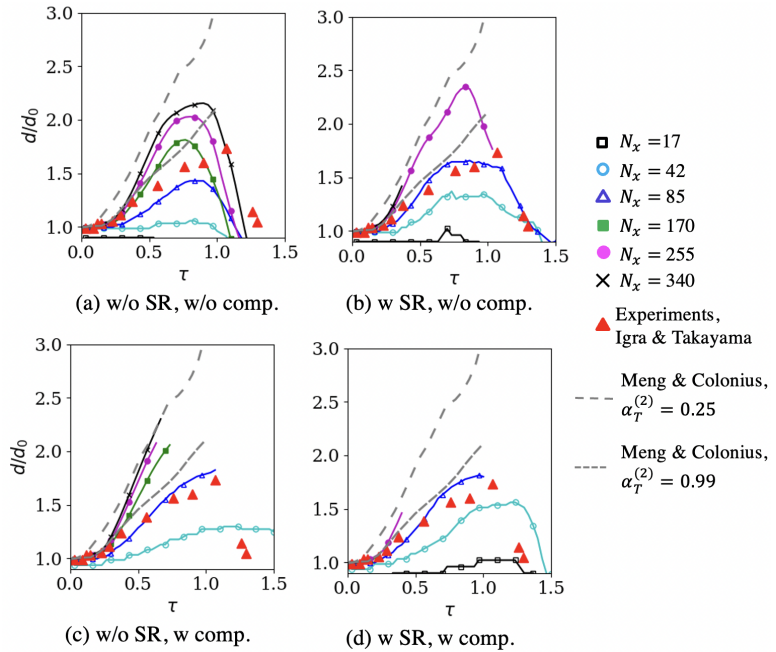


Figure 7: Time-evolution of the droplet height (d) compared against the experimental measurements [24] and a previous numerical study [21].

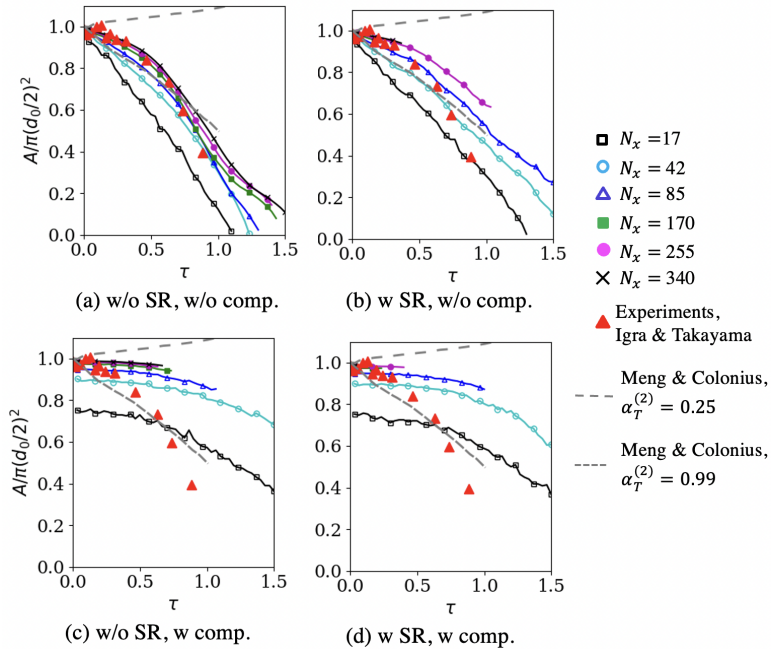


Figure 8: Time-evolution of the droplet area (A) compared against the experimental measurements [24] and a previous numerical study [21].

et al. [15] was required [26]. The six-equation model was able to accurately model the collapse and the rebound of the bubble, however, only when the pressure relaxation terms (R_p^κ) are included [25]. Since the previous tests in this work have shown the ability of the DEM within the seven-equation framework to relieve the need to use the SR, this configuration is simulated to evaluate if the same holds true here.

Considering the high computational cost of simulating the entire spherical droplet, a 3D spherical sector with 5° angle is used as the computational domain. The phase (1), i.e., the bubble, is modeled as CPG with $\gamma^{(1)} = 1.4$, whereas the phase (2), i.e., the surrounding water, is modeled as SG with $\gamma^{(2)} = 2.35$, $p_0^{(2)} = 1 \times 10^9$ Pa [25]. Initially, $\alpha^{(2)} = \epsilon$ for $r < r_0$ and $\alpha^{(2)} = 1 - \epsilon$ for $r \geq r_0$, where r_0 is the initial bubble radius. The pressure within the bubble is set as $p^{(1)} = p^{(2)} = p_b$, and it relaxes in the radially outward direction to p_∞ as $p^{(1)}(r) = p^{(2)}(r) = p_\infty + \frac{r_0}{r}(p_b - p_\infty)$. Here, r is the distance from the center of the bubble. To avoid any effects of the outer boundary, the computational domain radially extends from $r = 0.01r_0$ to $r = 32r_0$. Symmetry boundary conditions are used in the azimuthal direction and at $r = 0.01r_0$. A Neumann boundary condition is used for $r = 32r_0$.

The grid contains of $1000 \times 4 \times 4$ cells, with uniform cells of size $r_0/100$ distributed in the radial direction for $r < 2r_0$ and gradual coarsening in the outer region. This grid resolution is consistent with the previous works [25, 26]. Two pressure ratios, i.e., $p_\infty/p_b = 10, 1427$, are considered [26]. The simulation results are compared against the semi-analytical solution obtained using the Keller–Miksis equation [28], which is a compressible form of the Rayleigh–Plesset equation. This equation uses an asymptotic expansion in Mach number for a spherical bubble, so its use here as the exact solution presumes that errors measured relative to it are larger than any errors associated with the asymptotic expansion and presumption of sphericity inherent to it.

The simulation results with the seven-equation model are shown in Fig. 9. Due to the higher pressure in the surrounding liquid, the bubble starts collapsing and the pressure inside it starts to increase. Once the pressure inside the bubble gets higher than the surrounding, it starts to rebound and the pressure inside starts relaxing. For both $p_\infty/p_b = 10, 1427$, the simulations that employ the SR are able to model the collapse and the rebound of the bubble. On the other hand, the simulation results without the SR are able to predict the bubble collapse accurately, but not its rebound. Additional simulations are considered where we employ the SR for the pressure but not for the velocity, and these simulations are also able to accurately predict the bubble collapse-rebound process for both p_∞/p_b , reconfirming the importance of maintaining the pressure equilibrium between the phases for this case.

Considering the interchangeable roles of the non-conservative interphase exchange terms I^κ and the relaxation terms R^κ , one would expect the simulations even without the SR terms to capture the collapse-rebound process if I^κ are modeled accurately. Previous tests with shock interactions showed this. To further understand this behavior, additional simulations with finer grids (2000, 4000 cells in the radial direction) are conducted for $p_\infty/p_b = 10$ without the SR, and these do approach towards the semi-analytical solution. This suggests that similar to the other tests considered in this work, even for this challenging problem, where modeling the effects of pressure equilibrium is crucial, the DEM can handle the pressure equilibrium through the interface terms I^κ , relieving the need to model R^κ , but it requires a much higher resolution. A similar grid refinement study can also be considered for $p_\infty/p_b = 1427$, but since the collapse-rebound process for that is much sharper, and the minimum radius is even smaller, it is expected that simulating this without the SR would require a tremendous resolution. In this context, including the pressure SR for such a problem is suggested with the seven-equation model.

Corresponding modifications are included in the revised manuscript on page 3, Table 2 on page 18, Section 4.7 on page 31, 32, Figure 19 on page 33, and conclusions on page 40 (line 966).

- For some cases, SR/interface compression seem to be beneficial for others not. Thus, it is hard to tell when to use it beforehand? In particular, I understand that viscosity can only be verified using interface compression, however, the aerobreakup tests indicate limited applicability of IC. Please comment on possibilities to create a general setup for multi-component simulations.

We thank the reviewer for this question as it would further strengthen the novel contributions of this work. The below modifications are made in the revised manuscript in the conclusions on page 39, 40

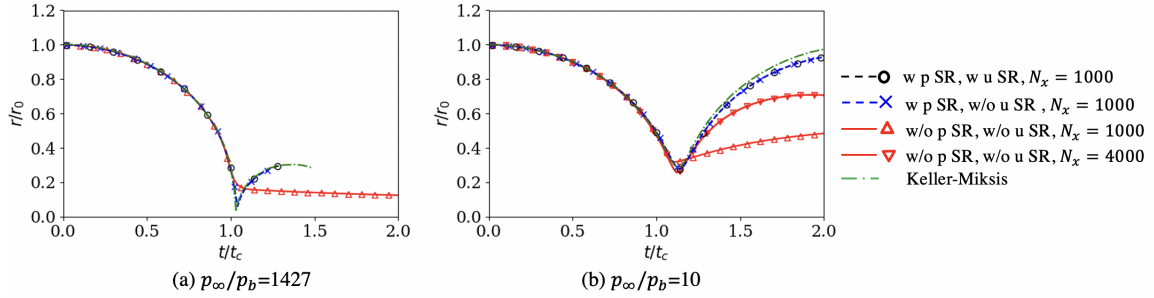


Figure 9: Bubble radius evolution is plotted during the spherical bubble collapse for two p_∞/p_b and various combinations of using the stiff relaxation (SR) solver for the pressure (p) and the velocity (u). Higher grid resolutions are also shown for $p_\infty/p_b = 10$ without the SR. N_x refers to the number of cells in the radial direction. The results are compared against the semi-analytical solution of Keller and Miksis [28].

(line 959-978).

- A stiff relaxation (SR) solver is often needed to enforce the pressure and the velocity equilibrium between the phases at the interface [10]. Since both the interface terms I^κ and the relaxation terms R^κ model interphase exchanges at the interface, with accurate modeling of I^κ using the DEM [2], the need of SR is relieved for most tests (i.e., shock-tube, shock-impact, viscous drag). The surface tension test shows inaccurate results with the SR, as enforcing a pressure jump between the phases creates an artificial pressure-jump in the DEM-based Riemann sub-problems. On the other hand, for predicting collapse-rebound of a spherical bubble, pressure SR (R_p^κ) is still needed with coarse grids, and modeling this without the SR, i.e., only through I^κ , requires a significantly higher grid resolution. A generalized approach may have to be devised in the future which either relieves the need to use the pressure SR even for challenging problems such as a spherical bubble collapse at reasonable grid resolutions, or allows its use in presence of surface tension.
 - An interface compression scheme initially used for the five-equation model is modified for the seven-equation model. The interface compression was necessary for the surface tension tests and the viscous drag computation. Otherwise, the droplet interface gets irregular, leading to difficulties in curvature computation and boundary and shear layer predictions surrounding the droplet surface. However, the interface compression scheme was detrimental for the 2D shock-droplet interaction, since it would treat the dispersed phase regions with unresolved MPEs as numerically diffused regions and apply compression. An interface compression scheme should still be used for resolved MPE modeling, however, a hybridization approach should be considered in the future so that it is dynamically switched off in regions with unresolved MPE.

Some additional minor comments:

- Table 1: Arbitrary EOS, viscosity and interface compression are discussed in this manuscript. Shouldn't it be P then instead of PNA for the 7-eq DIM?

We have clarified in the revised manuscript on Page 4, Table 1 caption that PNA refers to the features that are possible, but not attempted prior to this work. These have been addressed in the current work.

- p.4 additional (EOS) in line 8.

This typo has been fixed now on page 5 above line 153 of the revised manuscript.

- I understand that S_K and v_{im} are discussed later in the section. However, they should be introduced/named directly after equation 2.2/2.3 to avoid any confusion.

We thank the reviewer for this comment. They have been introduced now on page 4 after equations 2.2, 2.3 in the revised manuscript (line 148-149).

- The mathematical formula for heat flux is provided together with a fixed Prandtl number. Is it used in any of the test cases? If it is only applied in the last test case, you could also consider to provide the exact numbers there.

The heat flux is used for tests in Section 4.6 that validate the viscous effects. However, we still provide all the details in the formulation section for completeness. No corresponding modifications are made in the revised manuscript.

- Table 2: Dimensionality of the cases could be added. While EOS, surface tension, viscosity are real features, droplet deformation does not really fit this line. Pulse advection only tests the linear behavior of the solver.

The dimensionality of the cases is now added in Table 2 on page 18 in the revised manuscript. It is also clarified that the advection test only captures the linear behavior of the solver. We thank the reviewer for these suggestions. We agree that droplet deformation is not a new feature of the model, however, being able to model the deformation of the droplet in presence of a shock is an important ability that the model should possess. Corresponding changes are reflected in the revised manuscript on page 17 (line 435), and Table 2 on page 18.

- 4.1 Convection: Shouldn't it be advection? Also the given sine wave formula seems wrong. The values are just between 0.25 and 0.75 and the frequency does not make sense for the given domain. Why are there nonuniform jumps in the resolution (also for later cases) from 20 to 50 and then doubling afterwards? One flow through time might also be too short, can you redo your analysis for 5 or 10 t_f ?

We have replaced the word convection with advection now. To define the volume fraction as a smooth function that stays far from 0 and 1 (for avoiding any potential numerical errors due to division by zero), it is varied between 0.25 and 0.75 using a sine function as $\alpha^{(1)}(x) = (1/4) \sin(2\pi x/L) + 1/2$. The typo in the frequency is fixed now. We have now repeated this test for 14 flow-through times, and using finer grids than before. Uniform jumps in the grid resolution are chosen now. Corresponding changes are made in the revised manuscript on page 17 (line 449, 450), page 19 (line 457), and Figure 5.

- Eq. 4.1.: I guess a square is missing in the error formulation for the L2-norm.

This has been fixed in the revised manuscript in Equation 4.1, Page 19.

- Fig. 5: volume fraction L_2 error could be added in the caption for the convenience of the reader.

The caption for Figure 5 now clarifies this in the revised manuscript .

- Units: Some cases are given with units [4.1: 1m etc.], others not [4.1 p_0 , 4.2 densities]. Maybe units can be ignored completely for the basic numerical tests. In case 4.4, [kg/s] seems wrong for densities.

We thank the reviewer for this noting this. Ours is a dimensional solver, and therefore, the units are added for all cases now to be consistent. The changes are included in the revised manuscript in Section 4.1 (page 19, line 453), 4.2 (page 20, line 499), and 4.4 (page 24, line 645, 646).

- Figure 7.: Please indicate the difference in the setting of the first and second row since the captions are the same.

This has been fixed in Figure 7 in the revised manuscript.

- Case 4.3.: The malfunction of epsilon 10^{-3} seems trivial since for such an high epsilon value the density would be dominated by the heavy phase even in the pure gas region? How did the results look like for an initial shock wave in Al? Could you provide the applied material parameter for the HMX case.

The objective of showing results for $\epsilon = 10^{-3}$ was to understand differences between IC-1 and IC-6, one that uses the SR and the other does not. The results for a shock that was initiated in Al are now added in the revised manuscript page 21, 22 (line 554-559) and Figure 8. These are repeated below. It is not clear what the reviewer refers to by the applied material parameter. Further details about the MG EOS for HMX can be found elsewhere [29].

To initiate the shock in Aluminum, the driven section is set to $p^{(1)} = p^{(2)} = 10^5$ Pa, the driver section is set to $p^{(1)} = p^{(2)} = 10^7$ Pa; and $u^{(1)} = u^{(2)} = 0$ m/s, $\rho^{(1)} = 1.2$ kg/m³, and $\rho^{(2)} = 2784$ kg/m³ are

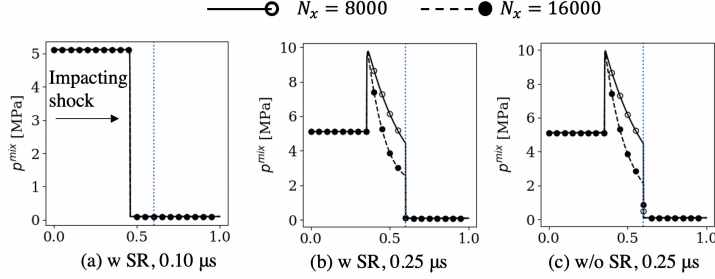


Figure 10: The p^{mix} is shown for the 1D shock interacting with Al/Air material interface. The vertical dashed line shows the location of the material interface. The results shown here are with the second-order scheme.

set everywhere in the domain. The results are shown in Fig. 10. The transmitted wave is a shock (not noticeable here), and the reflected wave is a rarefaction as expected due to the lower impedance of the air compared Aluminum [18]. Capturing the reflected rarefaction wave requires a fine grid, and the results are still similar with or without the SR. An exact solution was not available at these conditions for a comparison.

- Case 4.4 2: Fig. 9: Should it be $t=0.034$?

This typo has been fixed in the revised manuscript in Figure 9.

- Fig. 10: Please indicate which phase is gas/liquid. Different applied scales for the above row could be misleading. Why does the pressure initially reduce in the gas phase?

Fig. 14 in the revised manuscript is updated to reflect these clarifications.

- Case 4.5: Fig 13. Which exact position within the domain is plotted? Please specify the exact boundary condition for the second case. Does the observed eddy frequency match the expected value?

There was an error on the axis-labels for this figure. Fig. 17 in the revised manuscript is updated correspondingly and the entire computational domain is shown. The boundary conditions are now specified on 30 of the revised manuscript.

During the quasi-steady behavior, i.e., $t/t_0 > 15$, the shedding frequency is predicted as 308 Hz. Due to the flattening of the droplet, the effective diameter that the incoming flow sees is $1.17d_0$. Correspondingly, the Strouhal number (St) is predicted as 0.18, which is close to the experimental value ≈ 0.2 reported for a solid cylinder at $Re \approx 813$ [30]. These details are mentioned on the Page 30 (line 733-735) of the revised manuscript.

- Case 4.6: Is there a reason why the coarse grid is used for presentation in Fig. 16? It would have been more interesting to present the higher resolved case for $D=340$.

These results were shown for $N_x = 83$ to allow for a qualitative comparison against those of Meng and Colonius [21] that were obtained with the five-equation model and $N_x = 100$. This is now clarified on page 33 (line 813) in the revised manuscript.

- Case 4.7.: You mention that SR/IC has been tested, however, what are the results of it? Are there significant differences? Are the presented results qualitatively correct? The quality of the simulation is hard to estimate if there is no reference at all.

Unfortunately, in absence of any available data, it was not possible to present an experimental or numerical validation for this test. This limitation is reflected in Section 4.9 of the revised manuscript in the first paragraph (page 38, line 889). The simulation results with SR/IC showed qualitatively similar results, but in absence of any data for a quantitative comparison, no strong conclusions could be made.

Response to reviewer #2

This paper presents a seven-equation diffuse interface numerical method to model resolved compressible multiphase flows. The authors develop a 3D finite volume method following work in the literature, in particular the DEM method of [2]. The computational model includes viscosity effects, surface tension, and can handle arbitrary equations of state. Several challenging numerical tests show the effectiveness of the method. I think that this work is very interesting. Although the novel contributions are limited, I think that this article might deserve publication in the Journal of Computational Physics, provided the authors address the questions and comments below.

We thank the reviewer for all the constructive comments, and the revisions, we believe have improved the readability and the technical content of the manuscript. All added clarifications to the points raised are indicated in blue in the manuscript. The novelty statement is revised based on the comments from this as well as the other reviewers (see line 72-106 on page 3 of the revised manuscript).

- Table 1, p. 3, I think that it is confusing to indicate “Not Possible” for “Arbitrary EOS” for the five-equation DIM model. In fact one can use arbitrary EOS for the two phases of the five-equation model, which then determine the mixture equilibrium pressure. Perhaps the authors intend “Arbitrary EOS with independent phase pressure evolution”, but this should be clarified.

We apologize for the confusion in the terminology. It is true that the five-equation model can work with arbitrary equation of state (EOS), however, it requires building a mixture EOS, and this is not possible when the forms of the EOS are arbitrarily different for the phases. For example, one phase modeled with a stiffened gas (SG) EOS and another phase modeled with a thermally perfect gas (TPG) EOS. This capability of ‘arbitrarily independent forms of EOS’ may also be of interest when only a tabular EOS is available for one or more phases.

This is clarified in the revised manuscript on page 3 (line 77) and page 4 in Table 1, page 38 (line 924).

- The authors say that the use of DEM relieves the need to use a stiff relaxation solver because of the accurate modelling of the non-conservative fluxes. I think that the authors should add some discussion about the ability/inability of other methods for the 7-equation model to provide the same performance. For instance the method in HLLC-type Riemann solver with approximated two-phase contact for the computation of the Baer-Nunziato two-fluid model [31] appears to be able to relieve the need to use a stiff relaxation solver, based in particular on the 1D test in Fig. 12.

We thank the reviewer for directing us to these other works. The differences between the DEM and these other methods in terms of their ability/inability to use the 7-equation model with/without the stiff relaxation solver are identified as below. This discussion is added in the revised manuscript on page 2 (line 36-54), page 3 (119-120) in the introduction

For DIM, and particularly for the seven-equation model, modeling of the non-conservative terms have presented several challenges. Saurel and Abgrall [10] used a HLL Riemann solver and Andrianov and Warnecke [32] used an exact solution of a linearized Riemann solver for the conservative terms, while using the ‘free-stream’ condition to guide modeling of the non-conservative terms. Schwendeman et al. [33] developed an iterative Riemann solver and modeled the multiphase interface as of vanishingly small thickness with a smooth solution to model both the conservative and the non-conservative terms. Lochon et al. [31] used a HLLC Riemann solver but with an approximation for the two-phase contact. Taking a different route, Abgrall and Saurel [2] developed the discrete equations method (DEM), where instead of solving the two-phase problem Riemann problem with the phase volume-fraction as a variable, multiple Riemann sub-problems are solved with only pure phase phases as its left- and right-states. Modeling of both conservative and non-conservative terms naturally followed.

Even though the original work by Saurel and Abgrall [10] used a relaxation step to enforce pressure and velocity equilibrium between the phases, it was shown later that with the use DEM [2], since the non-conservative terms are computed accurately, the interphase exchange processes are accurately captured and the pressure- and the velocity-equilibrium can be maintained at the interface even without the relaxation step. Some other works, that computed the non-conservative terms accurately [31, 33], also

did not need a relaxation step, although these were limited to 1D shock-tube configurations. This effect is further studied in this work for more complex problems.

- Concerning the development of the HLLC-type Riemann solver that includes surface tension, the authors should cite at least the article below that develops a similar HLLC-type Riemann solver with surface tension for another multiphase compressible flow model, and comment on the differences: Towards sodium combustion modeling with liquid water [34].

We thank the reviewer for directing us to this recent work. As noted earlier, DEM [2] is used in this work for computing the conservative and the non-conservative terms, where instead of solving the two-phase problem Riemann problem with the phase volume-fraction as a variable, multiple Riemann sub-problems are solved with only pure phase phases as its left- and right-states. Parallel to the development reported in this work, Furfaro et al. [34] considered similar modifications to the HLLC Riemann solver for inclusion of surface tension, and even though the derivation has similarities, the modifications in the current work are in the context of solving a (1)-(2) (i.e., gas-liquid) Riemann subproblem within the DEM, and not for a two-phase Riemann problem [34] with phase volume fraction as a variable.

This difference is clarified and the work by Furfaro and Saurel [35] is acknowledged in the revised manuscript on page 4 (line 126-130) and 9 (line 243-248).

- Fig. 7 p. 20, probably one row of results should be labeled w/o SR instead of w SR?

This has been corrected in Fig 7 of the revised manuscript.

- I think that the authors should cite additional work on the 7-equation model, for instance the one above [31] and The Riemann problem and a high-resolution Godunov method for a model of compressible two-phase flow [33]. The Riemann problem for the Baer-Nunziato two-phase flow model [32].

These works, i.e., Lochon et al. [31], Schwendeman et al. [33], Andrianov and Warnecke [32] and their similarities/differences with our work are now clarified in the revised manuscript on page 2 (line 38-54). Please also see our response to the second comment from this reviewer above in this regard. We thank the reviewer for directing us to these other works.

Response to reviewer #3

This manuscript presents an implementation of a seven-equation diffuse interface method and includes effects of surface tension, viscosity, multi-species, and reactions. The seven-equation model analytically allows for non-equilibrium of pressure and momentum. The authors describe two procedures for numerically enforcing equilibrium of pressure and momentum. The first procedure uses stiff pressure and velocity relaxation solvers, and the second procedure uses the discrete equations method (DEM) to properly model the non-conservative fluxes. Through multiple test cases, the procedures for numerically enforcing pressure and momentum equilibrium between phases were compared and the DEM method was shown to be more efficient and robust. The manuscript is well written. However, a critical issue is regarding a close similarity between this work and the work of Tiwari et al (see below) which was apparently overlooked in the manuscript. Additional issues exist around the topic of conservation. Publication of the manuscript is not recommended unless the following criticisms can be addressed:

We thank the reviewer for all the constructive comments, and the revisions, we believe have improved the readability and the technical content of the manuscript. All added clarifications to the points raised are indicated in magenta in the manuscript. We have taken particular care to address concerns from this and the other reviewers on the novelty of this work and its similarity with Tiwari et al. [1] as detailed below. Please refer to our response to the first comment from this reviewer below in this regard.

- In this work, the authors propose the use of a seven-equation model along with the non-conservative interface compression terms from Shukla et al. [36] for the volume-fraction equation. If one starts with this set of equations and analytically perform the relaxation procedure, the system of equations will reduce to the five-equation model with consistent terms in all the equations in Tiwari et al. [1]. Therefore, in terms of fidelity, the numerical procedures presented in this work should be similar to the work of Tiwari et al. [1], which is apparently overlooked by the authors. It is also quite possible that even in terms of quantitative predictions the two models generate very close or even identical results. In terms of numerical cost, the model in Tiwari et al. [1] takes care of relaxation analytically, and thus is likely to provide simpler and cheaper simulations. So the authors are recommended to analyze/highlight the differences in their current work with that of Tiwari et al. [1], and give an argument on the advantages of their numerical procedure over Tiwari et al. [1].

The use of reduced approaches (e.g., five-equation model as in Tiwari et al. [1]) is well-established for modeling resolved multiphase entities (MPE) using diffused interface method (DIM). However, unlike the reduced models (e.g., [1]), the focus of this work is the seven-equation model that carries phase-independent pressures and velocities. The benefits of carrying phase-independent pressures are robust representation strong shocks and large density ratios, and the ability to use arbitrarily independent forms of the EOS for the phases, and carrying phase-independent velocities allows representation of both resolved and unresolved multiphase entities within the same modeling framework that would be beneficial for modeling dense-to-dilute multiphase flows.

Such a capability can be of interest for dense-to-dilute multiphase modeling, e.g., liquid fuel injection [5], multiphase explosions [6], etc., where it is not computationally feasible to resolve all the small-sized MPEs (size \sim nm- μ m), but in other dense regions of the flow, certain multiphase features (size \sim mm-m) have to be resolved (e.g., for modeling primary breakup). Various algorithms that consider a rule-based transition between the vastly different resolved and dispersed phase approaches exist [7-9], however, unlike those, the seven-equation model will allow to handle both resolved and dispersed consistently within the same numerical framework with only minor changes related to the modeling of the relaxation terms. To demonstrate the unique potential of the more generalized seven-equation model, a new test (Section 4.4 in revised manuscript) is considered now. This contains unresolved particles in one part of the domain and the velocity non-equilibrium is required for accurate modeling of particle dispersion, whereas, a resolved multiphase interface is present in the other part of the domain that is modeled via DIM. This would not have been possible with the reduced five/six-equation models that enforce the velocity equilibrium analytically. Next, to establish the use of the seven-equation model for modeling resolved MPEs, where the reduced models are already well-established, we have showed novel extensions to handle strong shocks and arbitrarily independent forms of EOS for the phases, viscous effects, surface tension, multiple species, and reactions within the same numerical framework. Here, the seven-equation

model provides benefits over the five-equation model here by relieving the need to build a mixture EOS and due to the increased robustness.

Corresponding changes are reflected in the revised manuscript on page-1 in the abstract, page-3 (line 72-86, 89-98, 99-109, 108-117) in the introduction, and page 38 (line 932), page 39 (line 938) page 40 (line 980-985) in the conclusions. Section 4.4 in the revised manuscript discusses results for the new test mentioned above. These results are colored in red as they are also in response to another comment from reviewer-1.

- Artificial terms for the compression of the interface thickness are included, but these terms are not in conservative form. Recent work Jain et al. [37] (already cited in the manuscript), has proposed similar procedures which are in conservative form. Was there any motivation to use the non-conservative form of the interface compression term?

As noted by the reviewer, an interface compression (or regularization) scheme, initially developed for the five-equation model [1, 36], is modified here to be used with the seven-equation model. The conservative form of this equation leads to spurious oscillations, and therefore, a non-conservative form was used [36]. We note that a particular focus here is on developing the seven-equation method to be used for modeling highly compressible flows and shocks. Considering this, we stay with DEM (and MUSCL interpolations) as the numerical scheme of choice and the interface compression scheme is chosen such that it can work independently of the other parts of the solver. Recently, Jain et al. [37] showed success with the conservative form, but for this they included the diffusion and the compression terms within the volume-fraction evolution equation and used a central differencing for the entire system of equations. Such an extension can be considered in the future for the DEM framework, but for this work, to handle the interface compression independently from flux computation, the non-conservative form of Shukla et al. [36] is retained.

This justification is added in the revised manuscript on page 4 (line 139-143), page 16 (line 382-387), and page 40 (line 984).

- The authors could evaluate the local and global conservation of mass and other quantities in the test cases considered in the paper.

With the non-conservative form of the interface compression used here, the errors in mass conservation are $\sim 0.2\text{-}2\%$ (for initial $\delta = 0.2\text{-}2.5$) for the standalone tests shown in Section 3.6 and $\sim 0.03\%$ for the DIM simulations with interface compression in Section 4.5. These are deemed reasonable for this work, but the authors agree that modifications for the conservative form of the interface compression scheme should be considered in the future. Unfortunately, we were not able to evaluate the conservation errors for the other tests in the paper that include inflow/outflow.

These details are clarified on page 16 (line 410-412) in the revised manuscript.

- It could be good to include a column for 4-eq DIM in Table 1.

We thank the reviewer for this suggestion. We have not included the following details in the revised manuscript on 2 (line 67-71) and in Table 1 on page 3.

Further down the hierarchy of the reduced BN models [38], there are also four- [39–42] and three-equation [43, 44] models, that, in addition to the pressure and the velocity equilibrium between the phases, also assume thermal, and both thermal and chemical equilibrium, respectively. However, their problems with handling large jumps in material properties and mixture EOS are well-known [10, 44], and therefore they are not discussed here further.

References

- [1] A. Tiwari, J. B. Freund, C. Pantano, A diffuse interface model with immiscibility preservation, *Journal of Computational Physics* 252 (2013) 290–309.
- [2] R. Abgrall, R. Saurel, Discrete equations for physical and numerical compressible multiphase mixtures, *Journal of Computational Physics* 186 (2003) 361–396.

- [3] R. Saurel, F. Petitpas, R. A. Berry, Simple and efficient relaxation methods for interfaces separating compressible fluids, cavitating flows and shocks in multiphase mixtures, *Journal of Computational Physics* 228 (2009) 1678–1712.
- [4] A. Panchal, S. Menon, A hybrid Eulerian-Eulerian/Eulerian-Lagrangian method for dense-to-dilute dispersed phase flows, *Journal of Computational Physics* 439 (2021) 110339.
- [5] S. V. Apte, P. Moin, Spray modeling and predictive simulations in realistic gas-turbine engines, in: *Handbook of Atomization and Sprays*, Springer, 2011, pp. 811–835.
- [6] F. Zhang, D. Frost, P. Thibault, S. Murray, Explosive dispersal of solid particles, *Shock Waves* 10 (2001) 431–443.
- [7] M. Herrmann, A dual-scale les subgrid model for turbulent liquid/gas phase interface dynamics, in: *ASME/JSME/KSME 2015 Joint Fluids Engineering Conference*, American Society of Mechanical Engineers, 2015, pp. V001T21A001–V001T21A001.
- [8] L. Han, X. Hu, N. A. Adams, Scale separation for multi-scale modeling of free-surface and two-phase flows with the conservative sharp interface method, *Journal of Computational Physics* 280 (2015) 387–403.
- [9] G. Tomar, D. Fuster, S. Zaleski, S. Popinet, Multiscale simulations of primary atomization, *Computers & Fluids* 39 (2010) 1864–1874.
- [10] R. Saurel, R. Abgrall, A multiphase godunov method for compressible multifluid and multiphase flows, *Journal of Computational Physics* 150 (1999) 425–467.
- [11] C.-H. Chang, M.-S. Liou, A robust and accurate approach to computing compressible multiphase flow: Stratified flow model and AUSM+-up scheme, *Journal of Computational Physics* 225 (2007) 840–873.
- [12] S. Tokareva, E. F. Toro, HLLC-type riemann solver for the Baer-Nunziato equations of compressible two-phase flow, *Journal of Computational Physics* 229 (2010) 3573–3604.
- [13] N. T. Nguyen, M. Dumbser, A path-conservative finite volume scheme for compressible multi-phase flows with surface tension, *Applied Mathematics and Computation* 271 (2015) 959–978.
- [14] A. Zein, M. Hantke, G. Warnecke, Modeling phase transition for compressible two-phase flows applied to metastable liquids, *Journal of Computational Physics* 229 (2010) 2964–2998.
- [15] A. Kapila, R. Menikoff, J. Bdzil, S. Son, D. S. Stewart, Two-phase modeling of deflagration-to-detonation transition in granular materials: Reduced equations, *Physics of Fluids* 13 (2001) 3002–3024.
- [16] X. Rogue, G. Rodriguez, J. Haas, R. Saurel, Experimental and numerical investigation of the shock-induced fluidization of a particles bed, *Shock Waves* 8 (1998) 29–45.
- [17] R. Saurel, A. Chinnayya, Q. Carmouze, Modelling compressible dense and dilute two-phase flows, *Physics of Fluids* 29 (2017) 063301.
- [18] P. Sridharan, T. L. Jackson, J. Zhang, S. Balachandar, Shock interaction with one-dimensional array of particles in air, *Journal of Applied Physics* 117 (2015) 075902.
- [19] C. T. Crowe, J. D. Schwarzkopf, M. Sommerfeld, Y. Tsuji, *Multiphase flows with droplets and particles*, CRC press, 2011.
- [20] H. Chen, Two-dimensional simulation of stripping breakup of a water droplet, *AIAA Journal* 46 (2008) 1135–1143.
- [21] J. Meng, T. Colonius, Numerical simulations of the early stages of high-speed droplet breakup, *Shock Waves* 25 (2015) 399–414.

- [22] K. W. Thompson, Time dependent boundary conditions for hyperbolic systems, *Journal of computational physics* 68 (1987) 1–24.
- [23] T. J. Poinsot, S. K. Lele, Boundary conditions for direct simulations of compressible viscous flows, *Journal of Computational Physics* 101 (1992) 104–129.
- [24] D. Igra, T. Ogawa, K. Takayama, A parametric study of water column deformation resulting from shock wave loading, *Atomization and Sprays* 12 (2002).
- [25] K. Schmidmayer, J. Caze, F. Petitpas, E. Daniel, N. Favrie, Modelling interactions between waves and diffused interfaces, *International Journal for Numerical Methods in Fluids* (2021) 1–27.
- [26] K. Schmidmayer, S. H. Bryngelson, T. Colonius, An assessment of multicomponent flow models and interface capturing schemes for spherical bubble dynamics, *Journal of Computational Physics* 402 (2020) 109080.
- [27] G. Allaire, S. Clerc, S. Kokh, A five-equation model for the simulation of interfaces between compressible fluids, *Journal of Computational Physics* 181 (2002) 577–616.
- [28] J. B. Keller, M. Miksis, Bubble oscillations of large amplitude, *The Journal of the Acoustical Society of America* 68 (1980) 628–633.
- [29] M. Akiki, T. P. Gallagher, S. Menon, Mechanistic approach for simulating hot-spot formations and detonation in polymer-bonded explosives, *AIAA Journal* 55 (2017) 585–598.
- [30] U. Fey, M. König, H. Eckelmann, A new strouhal–reynolds-number relationship for the circular cylinder in the range $47 \leq 2 \times 10^5$, *Physics of Fluids* 10 (1998) 1547–1549.
- [31] H. Lochon, F. Daude, P. Galon, J.-M. Hérard, HLLC-type Riemann solver with approximated two-phase contact for the computation of the baer–nunziato two-fluid model, *Journal of Computational Physics* 326 (2016) 733–762.
- [32] N. Andrianov, G. Warnecke, The riemann problem for the baer–nunziato two-phase flow model, *Journal of Computational Physics* 195 (2004) 434–464.
- [33] D. W. Schwendeman, C. W. Wahle, A. K. Kapila, The Riemann problem and a high-resolution Godunov method for a model of compressible two-phase flow, *Journal of Computational Physics* 212 (2006) 490–526.
- [34] D. Furfarò, R. Saurel, L. David, F. Beauchamp, Towards sodium combustion modeling with liquid water, *Journal of Computational Physics* 403 (2020) 109060.
- [35] D. Furfarò, R. Saurel, Modeling droplet phase change in the presence of a multi-component gas mixture, *Applied Mathematics and Computation* 272 (2016) 518–541.
- [36] R. K. Shukla, C. Pantano, J. B. Freund, An interface capturing method for the simulation of multi-phase compressible flows, *Journal of Computational Physics* 229 (2010) 7411–7439.
- [37] S. S. Jain, A. Mani, P. Moin, A conservative diffuse-interface method for compressible two-phase flows, *Journal of Computational Physics* 418 (2020) 109606.
- [38] H. Guillard, M. Labois, Numerical modelling of compressible two-phase flows (2006).
- [39] P. Gaillard, V. Giovangigli, L. Matuszewski, A diffuse interface lox/hydrogen transcritical flame model, *Combustion Theory and Modelling* 20 (2016) 486–520.
- [40] R. Saurel, P. Boivin, O. Le Métayer, A general formulation for cavitating, boiling and evaporating flows, *Computers & Fluids* 128 (2016) 53–64.
- [41] A. Chiapolino, P. Boivin, R. Saurel, A simple and fast phase transition relaxation solver for compressible multicomponent two-phase flows, *Computers & Fluids* 150 (2017) 31–45.

- [42] A. D. Demou, N. Scapin, M. Pelanti, L. Brandt, A pressure-based diffuse interface method for low-mach multiphase flows with mass transfer, *Journal of Computational Physics* 448 (2022) 110730.
- [43] E. Goncalves, R. F. Patella, Numerical simulation of cavitating flows with homogeneous models, *Computers & Fluids* 38 (2009) 1682–1696.
- [44] S. Clerc, Numerical simulation of the homogeneous equilibrium model for two-phase flows, *Journal of Computational Physics* 161 (2000) 354–375.